Chapter 1

The idea of a stochastic space-time: theory and experiments

M.Consoli and A.Pluchino

Istituto Nazionale di Fisica Nucleare, Sezione di Catania and Dipartimento di Fisica e Astronomia dell'Università di Catania

Contents

1. Introduction

There are two radically different ways to look at the origin of symmetries. On the one hand, for esthetic reasons, a symmetry could simply be postulated from scratch as, for instance, in the grand-unified scenarios of elementary particle physics. On the other hand, one could consider a symmetry as an *emergent* phenomenon [1]. From this latter point of view, the symmetry emerges from a microscopic description that, at the deepest level, does not know about its existence. In this sense, the emergence of symmetries could also be viewed as the tendency of physical systems toward self-organization and complexity [2].

As a definite example, one can consider the case of electromagnetism and Lorentz symmetry. At the end of XIX century, electromagnetic waves were described as hydrodynamic disturbances of an underlying ether represented, by Thomson, Fitzgerald and others, as an incompressible turbulent

fluid (a vortex 'sponge') [3]. The main point was that, due to the energy which is locally stored in the turbulent motion, on a coarse-grained scale, a fluid can start to behave as an elastic medium and thus support the propagation of transverse waves whose speed c_γ coincides with the average speed $c \equiv c_{\rm turbulence}$ of the chaotic internal motion of the elementary fluid constituents.

With the advent of Einstein's axiomatic approach, the ether started to be considered a superfluous concept. Still, as we shall review in Sect.2, the concept of the vacuum as an underlying turbulent ether is re-proposed by formal analogies with some foundational aspects of *both* quantum theory and relativity. This leads to the idea that space-time may have a fundamental stochastic nature.

Therefore one may ask: beyond the simple level of a formal analogy, there could be some definite experimental signature for this type of picture? This possibility will be considered in Sects. 3−7 where we shall compare with the phenomenological aspects of the ether-drift experiments. In the framework of a Lorentzian form of relativity and by representing the physical vacuum as a stochastic medium, our numerical simulations indicate that all classical ether-drift experiments could become consistent with the average Earth's motion which today is used to characterize the anisotropy of the Cosmic Microwave Background (CMB). Finally, in Sect.8, the overall consistency of this view with the present ether-drift experiments and the need for a new generation of dedicated experiments will also be emphasized.

2. The physical vacuum as a form of turbulent ether

In this section, we shall list a few different motivations that might induce to represent the vacuum as a form of random medium which resembles a turbulent fluid.

a) At the dawn of XX century Lorentz symmetry was believed to emerge from an underlying ether represented, by Thomson, Fitzgerald and others, as an incompressible turbulent fluid (a vortex 'sponge') [3]. More recently, the turbulent-ether model has been re-formulated by Troshkin [4] (see also [5] and [6]) in the framework of the Navier-Stokes equation. The main point of these hydrodynamic derivations is that, due to the energy which is locally stored in the turbulent motion, on a coarse-grained scale, a fluid can start to behave as an elastic medium and thus support the propagation of transverse waves whose speed c_γ coincides with the average speed $c \equiv c_{\rm turbulence}$ of the chaotic internal motion of the elementary fluid constituents.

To understand intuitively why, on coarse-grained scale, a fluid can start to behave as a solid one can just think of jets of water of sufficient speed. However, this idea is also supported by the formal equivalence [7; 8] (velocity potential vs. displacement, velocity vs. distortion, vorticity vs. density of dislocations,...) that can be established between various systems of dislocations in an elastic solid and corresponding vortex fields in a liquid. In this sense, the phenomenon of turbulence provides a conceptual transition from fluid dynamics to a different realm of physics, that of elasticity. With this transition, the parameter c acquires also the meaning of a *limiting* speed for the motion of soliton-like dislocations taken as models of ordinary matter (see e.g. refs.[9; 10] and references quoted therein). This is due to the behaviour of their elastic energy which increases proportionally to $(1 - v^2/c^2)^{-1/2}$.

This perspective is similar to starting from the basic equation that determines the mutual variations of the energy E and the linear momentum $\mathbf{p} = M\mathbf{v}$ of a body

$$\frac{dE}{dt} = \mathbf{v} \cdot \frac{d(M\mathbf{v})}{dt} \tag{1}$$

and allowing for a v^2-dependence in M (see e.g. [11]). This gives

$$dE = \frac{1}{2} M dv^2 + v^2 dM \tag{2}$$

The main point is that, if ordinary matter were interpreted in terms of soliton-like excitations of an underlying turbulent ether, one now disposes of the velocity parameter $c \equiv c_{\text{turbulence}}$. Then, by setting $E \equiv c^2 M(v^2/c^2)$, one has $\frac{dE}{dv^2} = c^2 \frac{dM}{dv^2}$ and Eq.(2) becomes $\frac{dM}{dv^2}\left(c^2 - v^2\right) = \frac{1}{2}M$ Therefore, for $dM/dv^2 > 0$, c plays also the role of a limiting speed and one finally obtains

$$E = Mc^2 = \frac{M_0 c^2}{\sqrt{1 - v^2/c^2}} \tag{3}$$

On this basis, it becomes natural to introduce linear transformations of the four quantities E/c and $\mathbf{p} = M\mathbf{v}$ that preserve the quadratic combination $(E/c)^2 - \mathbf{p}^2 = (M_0 c)^2$ and thus, by starting from a microscopic turbulent-ether scenario, Lorentz symmetry could also be understood as an emergent phenomenon. In this interpretation, its ultimate origin has to be searched in the very existence of c and thus in the deepest random fluctuations of the fluid velocity, with time at each point and between different points at the same instant, that characterize a state of fully developed turbulence and provide a kinetic basis for the observed space-time symmetry [12].

Notice that, once Lorentz symmetry is an emergent property, c is only a limiting speed for those soliton-like, collective modes that, in an emergent interpretation, are taken as models of ordinary matter, e.g. vortices, elastic dislocations...Thus there is nothing wrong if the internal motion of the basic constituents takes place at an average speed c. At the same time, on the coarse grained scale which is accessible to physical rods and clocks, the basic constituents appear, so to speak, 'frozen' in the vacuum structure and only their collective excitations are directly observable. This means that, for the elementary ether constituents, Eq.(1) is now solved by the standard non-relativistic forms $E = \frac{1}{2}mv^2$ and $\mathbf{p} = m\mathbf{v}$, where m is the constituent constant mass.

b) As emphasized in ref.[13], this qualitative picture of the vacuum, as an underlying random medium, also arises from alternative views of the quantum phenomena as with stochastic electrodynamics [14]−[18] or Nelson's mechanics [19]. The former is essentially the classical Lorentz-Dirac theory with new boundary conditions where the standard vanishing field at infinity is replaced by a vacuum, random radiation field. This field, considered in a stationary state, is assumed to permeate all space and its action on the particles impresses upon them a stochastic motion with an intensity characterized by Planck's constant. In this way, one can get insight into basic aspects of the quantum theory such as the wave-like properties of matter, indeterminacy, quantization,... For instance, in this picture, atomic stability would originate from reaching that 'quantum regime' [16; 18] which corresponds to a dynamic equilibrium between the radiation emitted in the orbital motions and the energy absorbed in the highly irregular motions impressed by the vacuum stochastic field. In this sense, again, Lorentz' ether should not be thought as a stagnant fluid (for an observer at rest) or as a fluid in laminar motion (for an observer in uniform motion). Rather the ether should resemble a fluid in a chaotic state, e.g. a fluid in a state of turbulent motion. The same is true for Nelson's mechanics. Here, the idea of a highly turbulent fluid emerges if one uses Onsager's original result [20] that in the zero-viscosity limit, i.e. infinite Reynolds number, the fluid velocity field does not remain a differentiable function [a]. This provides a basis to expect that "the Brownian motion in the ether will not be smooth "[19] and thus to consider the particular form of kinematics which is at the basis of Nelson's stochastic derivation of the Schrödinger equation.

[a]Onsager's argument relies on the impossibility, in the zero-viscosity limit, to satisfy the inequality $|\mathbf{v}(\mathbf{x}+\mathbf{l}) - \mathbf{v}(\mathbf{x})| < (\text{const.})l^n$, with $n > 1/3$. Kolmogorov's theory [21] corresponds to $n = 1/3$.

c) At a more elaborate level, a qualitatively similar picture is also obtained by representing relativistic particle propagation from the superposition, at very short time scales, of non-relativistic particle paths with different Newtonian mass [22]. In this formulation, particles randomly propagate (in the sense of Brownian motion) in a granular medium which thus replaces the trivial empty vacuum [23]. The essential mathematical ingredient for this representation is the use of 'superstatistics' [24], intended as the superposition of several statistical systems that operate at different spatio-temporal scale, which is also known to provide a very good description of fluid particle trajectories in high Reynolds-number turbulence [25].

d) Finally, the idea of a fundamentally random vacuum is also motivated by quantum-gravity. According to this view, space-time, when resolved at very short distances, should exhibit quantum fluctuations and thus appear to be 'foamy' or 'spongy' in the sense of refs. [26; 27]. This original idea has lead to a very wide collection of ideas and intuitions including, for instance, the holographic principle (see [28] for a review), possible deformations of Lorentz symmetry (Doubly Special Relativity) [29] or models of dark energy and dark matter [30]. At the same time, coupling light and matter to a fluctuating metric leads to intrinsic limitations on the measurement of lengths [31; 32], to violations of the weak equivalence principle [33] and to an effective decoherence of quantum systems [34]. These effects can be used to restrict the possible quantum gravity models by comparing with the results of modern gravity-wave detectors [35] or with atomic interferometry [36] or with the beat signal of two ultrastable optical resonators [37]. What is relevant here for our purpose is that, as in the previous cases, the space-time foam of quantum gravity seems also to resemble a turbulent fluid. This idea, originally due to Wheeler [26], has been more recently exploited by Ng and collaborators [38] who have emphasized the close analogies between holographic models of space-time foam and the limit of turbulence for infinite Reynolds number. The main conclusion of these rather formal derivations is that the metric fluctuations in the holographic model, which give rise to length fluctuations $\Delta l \sim l^{1/3} l_{\rm planck}^{2/3}$, when compared with those in moving fluids, can also be interpreted as a manifestation of Kolmogorov's scaling law for velocity $\Delta v \sim l^{1/3}$ [21].

Thus, summarizing, from the old ether view to the present quantum-gravity models, there are several independent motivations to represent the physical vacuum as an underlying turbulent fluid. This non-trivial degree of convergence might originate from the fundamental nature of quantum gravity (e.g. from the correspondence between the metric fluctuations in

the holographic model and Kolmogorov's scaling law). However, one could also adopt the complementary point of view where instead the ubiquitous phenomenon of turbulence plays from the very beginning the most central role. In any case, it becomes natural to wonder whether this type of vacuum medium could represent the preferred reference frame of a Lorentzian approach and thus to look at the ether-drift experiments for possible experimental checks. At the same time, the non-trivial interplay between large-scale and small-scale properties of turbulent flows may induce one to re-consider some assumptions adopted so far in the interpretation of the data. These issues will be analyzed in detail in the following sections.

3. Ether-drift experiments, the velocity of light and the Lorentz invariance of the vacuum

Ether-drift experiments, where one attempts to measure an absolute velocity, are the only known experiments which, in principle, can distinguish Einstein's special relativity from the Lorentzian point of view with a preferred reference frame Σ. At the same time, by assuming the validity of Lorentz transformations, if the velocity of light c_γ propagating in the various interferometers coincides with the basic parameter c entering Lorentz transformations, relativistic effects conspire to make undetectable the velocity parameter V associated with the motion of a given frame S' with respect to Σ. Therefore the only possibility is that c_γ and c do not coincide *exactly*. In this case, in fact, the existence of a small mismatch would show up through a tiny anisotropy of the velocity of light, proportional to $(c-c_\gamma)/c$, which could be measured by rotating a Michelson interferometer.

To derive the relevant relation, we shall follow the same treatment given in ref.[39] which applies to light propagation in a dielectric medium when the refractive index $\mathcal{N} = 1+\epsilon$ is extremely close to unity. This is the case of the gaseous systems as air, helium,.., which were used in the classical ether-drift experiments (e.g. Michelson-Morley, Miller, Illingworth, Joos,...). For such systems, one can find a simple theoretical framework to analyze the experiments.

The standard assumption is that any anisotropy has to vanish when both the observer and the container of the medium are at rest in the hypothetical preferred frame Σ. Therefore, in the physical case where instead both the observer and the container of the medium are at rest in the laboratory S' frame, the anisotropy should vanish identically in the two limits when either $V = 0$ (i.e. $S' \equiv \Sigma$) or $\mathcal{N} = 1$ (i.e. when $c_\gamma \equiv c$). This means that, in a

power series expansion in the two small parameters $\beta = V/c$ and $\epsilon = \mathcal{N} - 1$, any possible anisotropy has to start to $\mathcal{O}(\epsilon\beta)$ for the one-way velocity $c_\gamma(\theta)$ and to $\mathcal{O}(\epsilon\beta^2)$ for the two-way velocity $\bar{c}_\gamma(\theta)$ (the only one that can be measured unambiguously) which, by its very definition, is invariant under the replacement $\beta \to -\beta$. At the same time, for any fixed β, $\bar{c}_\gamma(\theta)$ is also invariant under the replacement $\theta \to \pi + \theta$. Therefore, to the lowest non-trivial level $\mathcal{O}(\epsilon\beta^2)$, one can write down the general expression

$$\bar{c}_\gamma(\theta) = \frac{2c_\gamma(\theta)c_\gamma(\pi+\theta)}{c_\gamma(\theta)+c_\gamma(\pi+\theta)} \sim \frac{c}{\mathcal{N}}\left[1 - \epsilon\ \beta^2 \sum_{n=0}^{\infty} \zeta_{2n} P_{2n}(\cos\theta)\right] \qquad (4)$$

where, to take into account invariance under $\theta \to \pi + \theta$, the angular dependence is given as an infinite expansion of even-order Legendre polynomials with arbitrary coefficients $\zeta_{2n} = \mathcal{O}(1)$. In Einstein's relativity, where there is no preferred reference frame, these ζ_{2n} coefficients vanish exactly. In a Lorentzian relativity, consistently with Lorentz' point of view [44] "...it seems natural not to assume at starting that it can never make any difference whether a body moves through the ether or not..", there is no reason why they should vanish *a priori*. Therefore, one can adopt Eq.(4) and start to compare with experiments.

However, before analyzing its phenomenological implications, it is interesting to look for a possible dynamical mechanism which can explain the formal structure in Eq.(4). To this end, by following refs.[39; 40], one can explore the possible implications of those modern views where the vacuum state is usually represented (e.g. in the standard model) as originating from the macroscopic condensation of some elementary quanta in the same quantum state, say $\mathbf{k} = 0$ in some reference frame Σ. This characterizes the physically realized form of relativity and could play the role of preferred reference frame in a modern Lorentzian approach.

This possibility is usually not considered with the motivation, perhaps, that the average properties of the condensed phase are summarized into a single quantity which transforms as a world scalar under the Lorentz group, for instance, in the standard model, the vacuum expectation value $\langle\Phi\rangle$ of the Higgs field. However, this does not necessarily imply that the vacuum state itself has to be *Lorentz invariant*. Namely, Lorentz transformation operators U', U'',..could transform non trivially the reference vacuum state [b] $|\Psi^{(0)}\rangle$ (appropriate to an observer at rest in Σ) into $|\Psi'\rangle$, $|\Psi''\rangle$,.. (appro-

[b]We ignore here the problem of vacuum degeneracy by assuming that any overlapping among equivalent vacua vanishes in the infinite-volume limit of quantum field theory (see e.g. S. Weinberg, *The Quantum Theory of Fields*, Cambridge University press, Vol.II,

priate to moving observers S', S'',..) and still, for any Lorentz-invariant operator G, one would find

$$\langle G\rangle_{\Psi^{(0)}} = \langle G\rangle_{\Psi'} = \langle G\rangle_{\Psi''} = .. \tag{5}$$

Now, according to general quantum field theoretical arguments, deciding on its Lorentz invariance requires to consider the eigenvalues and the algebra of the *global* Poincaré operators P_α, $M_{\alpha,\beta}$ (α ,β=0, 1, 2, 3) where P_α are the 4 generators of the space-time translations and $M_{\alpha\beta} = -M_{\beta\alpha}$ are the 6 generators of the Lorentzian rotations. In this framework, exact Lorentz invariance of the vacuum requires to impose [39; 40] the problematic condition of a vanishing vacuum energy $E_0 = 0$. However, for interacting theories, with the exception of unbroken supersymmetric theories (which are not phenomenologically acceptable), there is no known way to ensure consistently the condition $E_0 = 0$. Thus the issue of an exact Lorentz invariant vacuum remains as an open problem which, at present, cannot be solved on purely theoretical grounds. Still, one can explore the possible observable implications. In fact, the simplest consequence of such non-invariance of the vacuum is an energy-momentum flow along the direction of motion with respect to Σ. This tiny flow, acting as an effective thermal gradient, could induce small convective currents of the molecules in weakly bound systems as gases. In this case, refracted light would exhibit a slight anisotropy which would produce *exactly* the same Eq.(4) [39].

In this scheme, one can also understand the difference [41; 42] with experiments performed in strongly bound systems, such as solid or liquid transparent media, as in the Shamir-Fox experiment [43]. Being aware that the classical experiments might also admit a non-null interpretation proportional to $(\mathcal{N} - 1)\beta^2$, they selected a medium where the effect of the refractive index could have been enhanced (i.e. perspex where $\mathcal{N} \sim 1.5$). Since this enhancement was not observed, they concluded that the experimental basis of Special Relativity was strengthened. However, with the proposed mechanism, in solid and liquid dielectrics one expects the small energy flow generated by the motion with respect to the vacuum condensate to mainly dissipate by heat conduction without generating any appreciable particle motion or light anisotropy in the rest frame of the medium. Thus one has a physical argument to reconcile the two different behaviours.

pp. 163-167).

The above non-trivial level of consistency motivates a new generation of precise ether-drift experiments where light propagates in weakly bound gaseous media which seem the best suited to detect the tiny energy-momentum flow associated with a Lorentz non-invariant vacuum state. In this respect, we observe that Eq.(4), in principle, is exact to the given accuracy and could be used for fits to the data where the first few ζ's are left as free parameters. This general structure can, however, be compared with the particular form (a pure second harmonic in θ) which is obtained by using Lorentz transformations to connect S to the preferred frame [c]

$$\bar{c}_\gamma(\theta) \sim \frac{c}{\mathcal{N}} \left[1 - \epsilon\beta^2 \ (a + b\sin^2\theta)\right] \tag{6}$$

with $a = 2$ and $b = -1$ which corresponds to setting $\zeta_0 = 4/3$, $\zeta_2 = 2/3$ and all $\zeta_{2n} = 0$ for $n > 1$ in Eq.(4). We can then define the anisotropy parameter $\mathcal{B}$

$$\frac{\bar{c}_\gamma(\pi/2+\theta) - \bar{c}_\gamma(\theta)}{\langle \bar{c}_\gamma \rangle} \sim \mathcal{B}\frac{v^2}{c^2}\cos 2(\theta - \theta_0) \tag{7}$$

where the pair (v, θ_0) describes the projection of $\mathbf{V}$ onto the relevant plane and

$$|\mathcal{B}| \sim \epsilon \tag{8}$$

Eq.(6) represents a definite realization of the general structure in (4) and a particular case of the Robertson-Mansouri-Sexl (RMS) scheme [45; 46] for anisotropy parameter $|\mathcal{B}| = \epsilon$. In this sense, it provides a partial answer to the problems posed by our limited knowledge of the electromagnetic properties of gaseous systems and will be adopted in the following as a tentative model for the two-way velocity of light.

To obtain an experimental check, let us adopt Eq.(6). Then, this anisotropy of the two-way velocity of light could be measured by rotating a Michelson interferometer. By assuming the validity of Lorentz transformations, in the rest frame S' of the apparatus, the length L of its arms does not depend on their orientation so that the interference pattern between two orthogonal beams of light depends on the time difference

$$\Delta T(\theta) = \frac{2L}{\bar{c}_\gamma(\theta)} - \frac{2L}{\bar{c}_\gamma(\pi/2+\theta)} \tag{9}$$

[c]We address the reader to ref.[39] for various details concerning the derivation of Eq.(6) (see in particular the Appendix A) or the exact relation between the value of the refractive index in the S' frame and its value when the container of the gas is at rest in the Σ frame.

In this way, by introducing the wavelength λ of the light source and the projection v of the relative velocity in the plane of the interferometer, one finds to order $\frac{v^2}{c^2}$ the fringe shift

$$\frac{\Delta\lambda(\theta)}{\lambda} \sim \frac{c\Delta T(\theta)}{\mathcal{N}\lambda} \sim \frac{L}{\lambda}\frac{v_{\rm obs}^2}{c^2}\cos 2(\theta-\theta_0) \tag{10}$$

In the above equation the angle $\theta_0 = \theta_0(t)$ indicates the apparent direction of the ether-drift in the plane of the interferometer (the 'azimuth') and the square of the *observable* velocity

$$v_{\rm obs}^2 \sim 2(\mathcal{N}-1)v^2 \tag{11}$$

is re-scaled by the tiny factor $2(\mathcal{N}-1)$ with respect to the true *kinematical* velocity $v^2(t)$.

Therefore, in this scheme, the interpretation of the experiments is transparent. According to Special Relativity, there can be no fringe shift upon rotation of the interferometer. In fact, if light propagates in a medium, the frame of isotropic propagation is always assumed to coincide with the laboratory frame S, where the container of the medium is at rest, and thus one has $v_{\rm obs} = v = 0$. On the other hand, if there were fringe shifts, one could try to deduce the existence of a preferred frame $\Sigma \neq S$ provided the following minimal requirements are fulfilled : i) the fringe shifts exhibit an angular dependence of the type in Eq.(10) ii) by using gaseous media with different refractive index one gets consistency with Eq.(11) in such a way that different $v_{\rm obs}$ correspond to the same kinematical v.

4. A fresh look at the classical ether-drift experiments

Before considering the classical ether-drift experiments, some introductory discussion is needed. These experiments were performed in a period when both relativity and quantum theory were not fully developed. Therefore, the theoretical model adopted to compare with the data was basically the old classical physics. In this interpretative scheme, the expected effects, although being formally $\mathcal{O}(v^2/c^2)$, were "large", as compared to the extraordinary sensitivity of the Michelson interferometer, and "smooth", because the only time dependence were due to slow effects such as the daily Earth's rotation and its annual orbital revolution.

To see this, let us first re-write the basic Eq.(10) as

$$\frac{\Delta\lambda(\theta)}{\lambda} \sim \frac{2L(\mathcal{N}-1)}{\lambda}\frac{v^2(t)}{c^2}\cos 2(\theta-\theta_0(t)) \equiv 2C(t)\cos 2\theta + 2S(t)\sin 2\theta \tag{12}$$

where (x-y denotes theplane of the interferometer)

$$C(t) = \frac{L(\mathcal{N}-1)}{\lambda}\frac{v^2(t)}{c^2}\cos 2\theta_0(t) = \frac{L(\mathcal{N}-1)}{\lambda}\ \frac{v_x^2(t)-v_y^2(t)}{c^2} \tag{13}$$

$$S(t) = \frac{L(\mathcal{N}-1)}{\lambda}\frac{v^2(t)}{c^2}\sin 2\theta_0(t) = \frac{L(\mathcal{N}-1)}{\lambda}\ \frac{2v_x(t)v_y(t)}{c^2} \tag{14}$$

Then, the standard classical assumption is to consider a cosmic Earth's velocity with well defined magnitude V, right ascension α and angular declination γ that can be considered constant for short-time observations of a few days where there are no appreciable changes due to the Earth's orbital velocity around the Sun. In this framework, where the only time dependence is due to the Earth's rotation, one identifies $v(t) \equiv \tilde{v}(t)$ and $\theta_0(t) \equiv \tilde{\theta}_0(t)$ where $\tilde{v}(t)$ and $\tilde{\theta}_0(t)$ derive from the simple application of spherical trigonometry

$$\cos z(t) = \sin\gamma\sin\phi + \cos\gamma\cos\phi\cos(\tau-\alpha) \tag{15}$$

$$\frac{\tilde{v}_x(t)}{V} \equiv \sin z(t)\cos\tilde{\theta}_0(t) = \sin\gamma\cos\phi - \cos\gamma\sin\phi\cos(\tau-\alpha) \tag{16}$$

$$\frac{\tilde{v}_y(t)}{V} \equiv \sin z(t)\sin\tilde{\theta}_0(t) = \cos\gamma\sin(\tau-\alpha) \tag{17}$$

$$\tilde{v}(t) \equiv \sqrt{\tilde{v}_x^2(t)+\tilde{v}_y^2(t)} = V\sin z(t), \tag{18}$$

Here $z = z(t)$ is the zenithal distance of $\mathbf{V}$, ϕ is the latitude of the observatory, $\tau = \omega_{\rm sid}t$ is the sidereal time of the observation in degrees ($\omega_{\rm sid} \sim \frac{2\pi}{23^h56'}$) and the angle θ_0 is counted conventionally from North through East so that North is $\theta_0 = 0$ and East is $\theta_0 = 90^o$. In this way, one finds

$$S(t) \equiv \tilde{S}(t) = S_{s1}\sin\tau + S_{c1}\cos\tau + S_{s2}\sin(2\tau) + S_{c2}\cos(2\tau) \tag{19}$$

$$C(t) \equiv \tilde{C}(t) = C_0 + C_{s1}\sin\tau + C_{c1}\cos\tau + C_{s2}\sin(2\tau) + C_{c2}\cos(2\tau) \tag{20}$$

In this picture, the C_k and S_k Fourier coefficients depend on the three parameters (V,α,γ) (see [39]) and, to very good approximations, should be time-independent for short-time observations.

However, this simple theoretical framework did *not* fit with the observations. In fact, the experimental data, even though slightly larger than the experimental resolution, were always much smaller than the expected size $\mathcal{O}(\beta^2)$. Also the observed pattern was highly irregular because observations

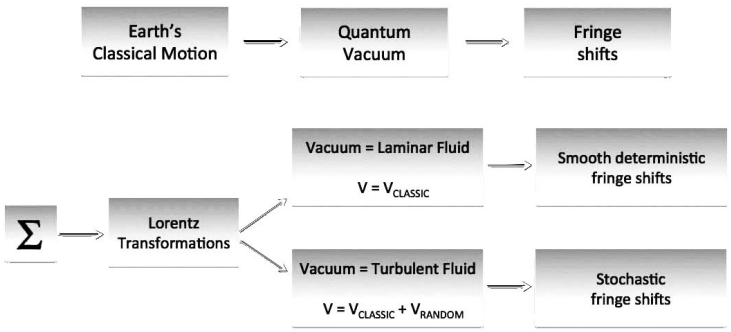

Fig. 1. The two possible ways to relate Earth's classical motion and fringe shifts.

performed at the same time on consecutive days could differ sizeably. This has always represented a strong argument to interpret the data as pure instrumental effects, i.e. "null results".

However, from time to time, greatest experts have seriously questioned this traditional null interpretation. Thus, one may ask if there could be some theoretical framework in which these "small" and "irregular" effects can acquire a definite physical meaning. For instance we have seen in Sect.2, see Eqs.(10) and (11), that, by assuming the existence of a preferred reference frame Σ and using Lorentz transformations (rather than Galileo's transformations), the expected effects would be proportional to $2(\mathcal{N}-1)\beta^2$ and *not* simply to β^2. Therefore, for instance, for air, where the refractive index $\mathcal{N}$ ∼1.00029, the fringe shifts for $V \sim 300$ km/s would be about 17 times smaller than those classical expected for $V \sim 30$ km/s. For gaseous helium, where $\mathcal{N} \sim 1.000035$, the effect would be even 140 times smaller.

In addition, there is another important aspect. By comparing the Earth's cosmic motion with that of a body in a fluid, the standard picture Eqs.(15)−(20) amounts to the condition of a pure laminar flow where global and local velocity fields coincide. Here, there is a logical gap. The relation between the macroscopic Earth's motions and the ether-drift experiments depends on the physical nature of the vacuum. If we consider the vacuum as a form of *quantum* ether, the fringe shifts will likely exhibit the typical irregular (non-deterministic) pattern which characterizes any quantum measurement. Therefore, from the theoretical arguments of Sect.2, rather than adopting the simple classical model of a laminar flow, one could try to compare the experimental data with models of a *turbulent* flow, see Fig.1.

In this case, due to the typical irregular behaviour, vectorial quantities (such as the fringe shifts) might easily average to zero. But, now, this does not mean that there is no ether-drift.

A complete analysis of all classical experiments was presented in ref.[39]. Here, we shall only restrict to the first, and most famous, experiment performed in 1887 by Michelson and Morley in Cleveland, and to the last, and most precise, version which was performed in 1930 by Joos in Jena. Due to the accuracy of this latter experiment we shall explicitly compare the data with numerical simulations of turbulent flows.

4.1. *Michelson-Morley*

Michelson and Morley performed their six observations in 1887, on July 8th, 9th, 11th and 12th, at noon and in the evening, in the basement of the Case Western University of Cleveland [47]. As well summarized by Miller in 1933 [48], "The brief series of observations was sufficient to show clearly that the effect did not have the anticipated magnitude. However, and this fact must be emphasized, *the indicated effect was not zero*". The same conclusion had already been obtained by Hicks in 1902 [49]: "..the data published by Michelson and Morley, instead of giving a null result, show distinct evidence for an effect of the kind to be expected". Quantitatively, the situation can be summarized in Figure 2, taken from Miller [48], where the values of the effective velocity measured in various ether-drift experiments are reported and compared with a smooth curve fitted by Miller to his own results as function of the sidereal time.

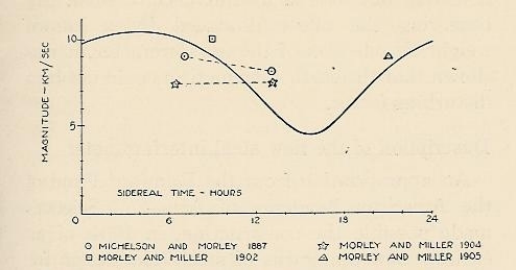

FIG. 4. Velocity of ether drift observed by Michelson and Morley in 1887, and by Morley and Miller in 1902, 1904 and 1905, compared with the velocity obtained by Miller in 1925.

Fig. 2. The magnitude of the observable velocity measured in various experiments as reported by Miller [48].

In the framework of Eq.(10), the fringe shift is a second-harmonic effect, i.e. periodic in the range $[0, \pi]$, whose amplitude A_2 is predicted differently by using the classical formulas or Lorentz transformations (10)

$$A_2^{\rm class} = \frac{L}{\lambda}\frac{v^2}{c^2} \qquad\qquad A_2^{\rm rel} = \frac{L}{\lambda}\frac{{v_{\rm obs}}^2}{c^2} \sim 2(\mathcal{N}-1)A_2^{\rm class} \quad (21)$$

Now, for the Michelson-Morley interferometer the whole effective optical path was about $L = 11$ meters, or about $2 \cdot 10^7$ in units of light wavelengths, so for a velocity $v \sim 30$ km/s (the Earth's orbital velocity about the Sun, and consequently the minimum anticipated drift velocity) the expected classical 2nd-harmonic amplitude was $A_2^{\rm class} \sim 0.2$. This value can thus be used as a reference point to obtain an observable velocity, in the plane of the interferometer, from the actual measured value of A_2 through the relation

$$v_{\rm obs} \sim 30 \sqrt{\frac{A_2}{0.2}} \ \ {\rm km/s} \quad (22)$$

For the Michelson-Morley experiment, the average observable velocity reported by Miller is about 8.4 km/s. Comparing with the classical prediction for a velocity of 30 km/s, this means an experimental 2nd- harmonic amplitude

$$A_2^{\rm EXP} \sim 0.2\ (\frac{8.4}{30})^2 \sim 0.016 \quad (23)$$

which is about twelve times smaller than the expected result.

Neither Hicks nor Miller reported an estimate of the error on the 2nd harmonic extracted from the Michelson-Morley data. To understand the precision of their readings, we can look at the original paper [47] where one finds the following statement: "The readings are divisions of the screw-heads. The width of the fringes varied from 40 to 60 divisions, the mean value being near 50, so that one division means 0.02 wavelength". Now, in their tables Michelson and Morley reported the readings with an accuracy of 1/10 of a division (example 44.7, 44.0, 43.5,..). This means that the nominal accuracy of the readings was ± 0.002 wavelengths. In fact, in units of wavelengths, they reported values such as 0.862, 0.832, 0.824,.. Furthermore, this estimate of the error agrees well with Born's book [50]. In fact, Born, when discussing the classically expected fractional fringe shift upon rotation of the apparatus by 90^o, about 0.37, explicitly says: "Michelson was certain that the one-hundredth part of this displacement would still be observable" (i.e. 0.0037). Therefore, to be consistent with

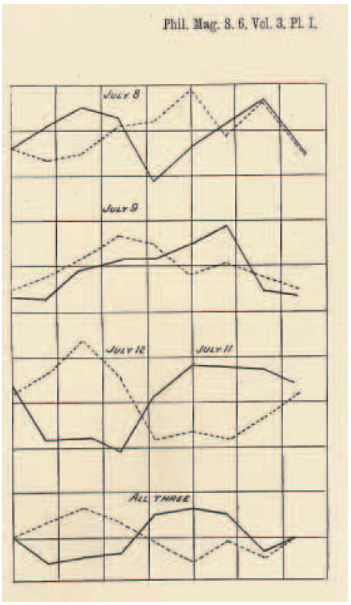

Fig. 3. The Michelson-Morley fringe shifts as reported by Hicks [49]. Solid and dashed lines refer respectively to noon and evening observations.

SESSION	A_2^{EXP}
July 8 (noon)	0.010 ± 0.005
July 9 (noon)	0.015 ± 0.005
July 11 (noon)	0.025 ± 0.005
July 8 (evening)	0.014 ± 0.005
July 9 (evening)	0.011 ± 0.005
July 12 (evening)	0.024 ± 0.005

both the original Michelson-Morley article and Born's quotation of Michelson's thought, the estimate ± 0.004 for the error was adopted in refs.[42; 39]. In these papers, many other details and all numerical values for the fringe shifts are reported.

The fringe shifts are given as a periodic function, with vanishing mean, in the range $0 \leq \theta \leq 2\pi$, so that they can be reproduced in a Fourier expansion. One can thus extract the amplitude and the phase of the 2nd-

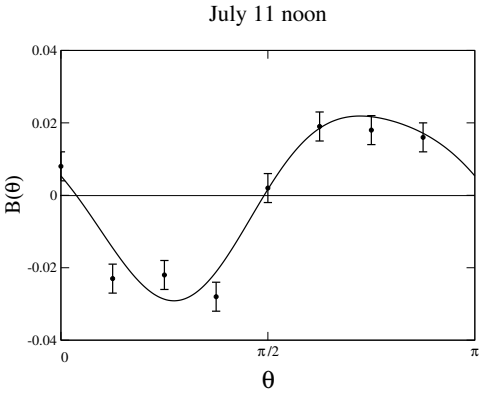

Fig. 4. A fit to the even combination $B(\theta)$ Eq.(24). The second harmonic amplitude is $A_2^{\rm EXP} = 0.025 \pm 0.005$ and the fourth harmonic is $A_4^{\rm EXP} = 0.004 \pm 0.005$. The figure is taken from ref.[42]. Compare the data with the solid curve of July 11th shown in Fig.3.

harmonic component by fitting the even combination of fringe shifts

$$B(\theta) = \frac{\Delta\lambda(\theta) + \Delta\lambda(\pi + \theta)}{2\lambda} \tag{24}$$

(see Fig.4). This is essential to cancel the 1st-harmonic contribution originally pointed out by Hicks [49]. Its theoretical interpretation is in terms of the arrangements of the mirrors and, as such, this effect has to show up in the outcome of real experiments. The 2nd-harmonic amplitudes from the six individual sessions are reported in Table 2. One can then compute the mean and variance of the six determinations reported in Table 2 by obtaining $A_2^{\rm EXP} \sim 0.016 \pm 0.006$. This value is consistent with an observable velocity $v_{\rm obs} \sim 8.4^{+1.5}_{-1.7}$ km/s. Then, by using Eq.(11), which connects the observable velocity to the projection of the kinematical velocity in the plane of the interferometer through the refractive index of the medium where light propagation takes place (in our case air where $\mathcal{N} \sim 1.00029$), we can deduce the average value

$$v \sim 349^{+62}_{-70}\ {\rm km/s} \tag{25}$$

While the individual values of A_2 show a reasonable consistency, there are substantial changes in the apparent direction θ_0 of the ether-drift effect in the plane of the interferometer. This is the reason for the strong cancelations obtained when fitting together all noon sessions or all evening sessions [52]. According to the usual interpretation, the large spread of the azimuths is taken as indication that any non-zero fringe shift is due to pure instrumental effects. However, as anticipated, this type of discrepancy could also

indicate an unconventional form of ether-drift where there are substantial deviations from Eq.(6) and/or from the smooth trend in Eqs.(15)−(18). For instance, in agreement with the general structure Eq.(4), and differently from July 11 noon, which represents a very clean indication, there are sizeable 4th- harmonic contributions (here $A_4^{\rm EXP} = 0.019 \pm 0.005$ and $A_4^{\rm EXP} = 0.008 \pm 0.005$ for the noon sessions of July 8 and July 9 respectively). In any case, the observed strong variations of θ_0 are in qualitative agreement with the analogous values reported by Miller. To this end, compare with Fig.22 of ref.[48] and in particular with the large scatter of the data taken around August 1st, as this represents the epoch of the year which is closer to the period of July when the Michelson-Morley observations were actually performed. Thus one could also conclude that individual experimental sessions indicate a definite non-zero ether-drift but the azimuth does not exhibit the smooth trend expected from the conventional picture Eqs.(15)−(18).

We emphasize that the large spread of the θ_0-values might also reflect a particular systematic effect pointed out by Hicks [49]. As described by Miller [48], " before beginning observations the end mirror on the telescope arm is very carefully adjusted to secure vertical fringes of suitable width. There are two adjustments of the angle of this mirror which will give fringes of the same width but which produce opposite displacements of the fringes for the same change in one of the light-paths". Since the relevant shifts are extremely small, "...the adjustments of the mirrors can easily change from one type to the other on consecutive days. It follows that averaging the results of different days in the usual manner is not allowable unless the types are all the same. If this is not attended to, the average displacement may be expected to come out zero − at least if a large number are averaged" [49].

Therefore averaging the fringe shifts from various sessions represents a delicate issue and can introduce uncontrolled errors. In fact, an overall change of sign of the fringe shifts at all $\theta-$values is equivalent to replacing the azimuth $\theta_0 \to \theta_0 \pm \pi/2$. However, this relative sign does not affect the values of A_2 and this is why averaging the 2nd-harmonic amplitudes in Table 1, as we have done, is a safer procedure. From these amplitudes one obtains the average kinematical velocity Eq.(25) which is completely consistent with the average value 369 km/s associated with the Earth's motion with respect to the CMB.

5. Numerical simulations in a turbulent-ether model

As anticipated at the end of Sect.4, identifying the local velocity field $(v_x(t), v_y(t))$ in Eqs.(12) $-(14)$ with the smooth, global quantities $(\tilde{v}_x(t), \tilde{v}_y(t))$ which describe the cosmic Earth's motion, is equivalent to adopt the model of a laminar flow. Instead, by adopting the different model of a turbulent flow, the situation changes completely.

As mentioned in the introduction, in the limit of vanishing viscosity, the local velocity field becomes non-differentiable. In these conditions, the ordinary formulation in terms of differential equations becomes inadequate and must be replaced by some other description such as a formulation in terms of random Fourier series [20; 53]. In this other approach, the parameters of the macroscopic motion are only used to fix the limiting boundaries [54] for a microscopic velocity field which has instead an intrinsic stochastic nature.

The simplest choice, which represents a zeroth-order approximation, corresponds to a turbulence which, at small scales, appears statistically isotropic and homogeneous [d]. In spite of its simplicity, it is a useful example to illustrate basic phenomenological features associated with an underlying stochastic vacuum. The perspective is that of an observer moving in the turbulent fluid who wants to simulate the two components of the velocity in his x-y plane at a given fixed location in his laboratory. In a statistically isotropic and homogeneous turbulence, one finds the general expressions

$$v_x(t) = \sum_{n=1}^{\infty} [x_n(1) \cos \omega_n t + x_n(2) \sin \omega_n t] \tag{26}$$

$$v_y(t) = \sum_{n=1}^{\infty} [y_n(1) \cos \omega_n t + y_n(2) \sin \omega_n t] \tag{27}$$

where $\omega_n = 2n\pi/T$, T being a time scale which represents a common period of all stochastic components. For our simulations, we have adopted the typical value $T = T_{\rm day}$= 24 hours. However, we have also checked with a few runs that the statistical distributions of the various quantities do not change substantially by varying T in the rather wide range $0.1\ T_{\rm day} \leq T \leq 10\ T_{\rm day}$.

The coefficients $x_n(i = 1, 2)$ and $y_n(i = 1, 2)$ are random variables with zero mean and have the physical dimension of a velocity. By assuming statistical isotropy, we shall denote by $[-\tilde{v}, \tilde{v}]$ the common interval for these

[d]This picture reflects the basic Kolmogorov theory [21] of a fluid with vanishingly small viscosity.

four parameters. In terms of $\tilde{v}$ the statistical average of the quadratic values can be expressed as

$$\langle x_n^2(i=1,2)\rangle_{\rm stat} = \langle y_n^2(i=1,2)\rangle_{\rm stat} = \frac{\tilde{v}^2}{3\ n^{2\eta}} \tag{28}$$

for the uniform probability model (within the interval $[-\tilde{v},\tilde{v}]$) which we have chosen for our simulations. Finally, the exponent η controls the power spectrum of the fluctuating components. For the simulations, between the two values $\eta = 5/6$ and $\eta = 1$ reported in ref.[54], we have chosen $\eta = 1$ which corresponds to the point of view of an observer moving in the fluid.

We observe that one could further improve the stochastic model by introducing time modulations and/or slight deviations from isotropy. For instance, $\tilde{v}$ could become a function of time $\tilde{v} = \tilde{v}(t)$. By still retaining statistical isotropy, this could be used to simulate the possible modulations of the projection of the Earth's velocity in the plane of the interferometer. Or, one could fix a range, say $[-\tilde{v}_x,\tilde{v}_x]$, for the two random parameters $x_n(1)$ and $x_n(2)$, which is different from the range $[-\tilde{v}_y,\tilde{v}_y]$ for the other two parameters $y_n(1)$ and $y_n(2)$. Finally, $\tilde{v}_x$ and $\tilde{v}_y$ could also become given functions of time, for instance $\tilde{v}_x(t) \equiv \tilde{v}(t)\cos\tilde{\theta}_0(t)$ $\tilde{v}_y(t) \equiv \tilde{v}(t)\sin\tilde{\theta}_0(t)$, $\tilde{v}(t)$ and $\tilde{\theta}_0(t)$ being defined in Eqs. (15)−(18). In this way, for each time t, Eqs.(28) now become

$$\langle x_n^2(i=1,2)\rangle_{\rm stat} = \frac{\tilde{v}_x^2(t)}{3\ n^{2\eta}} \qquad \langle y_n^2(i=1,2)\rangle_{\rm stat} = \frac{\tilde{v}_y^2(t)}{3\ n^{2\eta}} \tag{29}$$

For most classical experiments, these further refinements are unnecessary. In fact in most cases only observations at few selected hours were performed so that, in view of the strong fluctuations of the data, one can just extract the average magnitude of the observed velocity and, within the errors, a macroscopic kinematical velocity. A notable exception is Joos' 1930 experiment [55]. Its accuracy was incomparable among the classical experiments since the observations were performed each hour to cover the whole sidereal day and the data were recorded by photocamera. As we shall see in the next section, Joos' data are sensitive to the details of the Earth's cosmic motion and require to adopt the most refined framework Eqs.(29).

5.1. *Joos*

Joos' optical system [55] was enclosed in a hermetic housing and, traditionally, it was always assumed that the fringe shifts were recorded in a partial vacuum. On the other hand, Swenson [56] explicitly reports that fringe

shifts were finally recorded with optical paths placed in a helium bath. In spite of the fact that this important aspect is never mentioned in Joos' papers, we have followed Swenson by assuming that during the measurements the interferometer was filled by gaseous helium at atmospheric pressure.

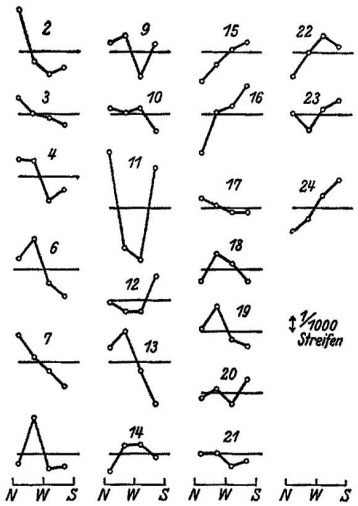

Fig. 8. Verschiebungen in einer über 24 Stunden erstreckten Serie beim Jenaer Versuch.

Fig. 5. The selected set of data reported by Joos [55]. The yardstick corresponds to 1/1000 of a wavelength so that the experimental dots have a size of about $0.4 \cdot 10^{-3}$. This corresponds to an uncertainty $\pm 0.2 \cdot 10^{-3}$ in the extraction of the fringe shifts.

The observations were performed in Jena in 1930 starting at 2 P.M. of May 10th and ending at 1 P.M. of May 11th. Two measurements, the 1st and the 5th, were finally deleted by Joos with the motivation that there were spurious disturbances. The data were combined symmetrically, in order to eliminate the presence of odd harmonics, and the magnitude of the fringe shifts was typically of the order of a few thousandths of a wavelength. To this end, one can look at Joos' picture (reported here as our Fig.5) and compare with the shown size of 1/1000 of a wavelength. From this picture, Joos decided to adopt 1/1000 of a wavelength as an upper limit and deduced an observable velocity $v_{\rm obs} \lesssim 1.5$ km/s. To derive this value, he used the fact that, for his apparatus, an observable velocity of 30 km/s would have produced a 2nd-harmonic amplitude of 0.375 wavelengths.

Still, since it is apparent from Fig.5 that some fringe displacements

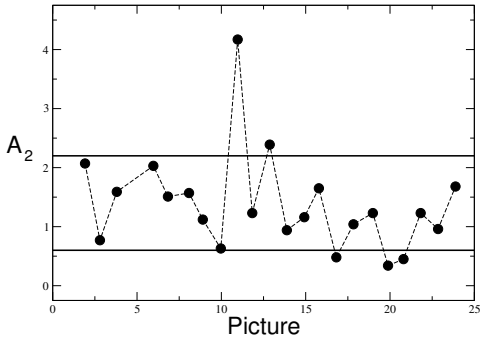

Fig. 6. Joos' 2nd-harmonic amplitudes, in units 10^{-3}. The vertical band between the two lines corresponds to the range $(1.4 \pm 0.8) \cdot 10^{-3}$. The figure is taken from Ref.[39].

were definitely larger than 1/1000 of a wavelength, the values of the 2nd-harmonic amplitude A_2 were extracted [39] from the 22 pictures. Differently from the values of the azimuth, this can be done unambiguously. The point is that, due to the camera effect, it is not clear how to fix the reference angular values θ_k in Fig.4 for the fringe shifts. In addition, there is a small misalignment angle, between the dots of Joos' fringe shifts and the N, W, and S marks, which cannot be deduced from the articles. Since clearly there is only one correct choice for the reference angles θ_k, we have preferred not to quote theoretical uncertainties on the azimuth and just concentrate on the amplitudes whose values, instead, do not depend on the angles θ_k and thus can be extracted unambiguously. Their values are reported in Fig.6. The accuracy of each determination is about $\pm 0.2 \cdot 10^{-3}$ as given by the size of Joos' experimental dots in Fig.5. This uncertainty is about one order of magnitude better than for Michelson-Morley and a factor of 3 better than the 1/1500 reading error in the Illingworth experiment [57].

By computing mean and variance of the individual values, we obtain an average 2nd-harmonic amplitude

$$\langle A_2^{\rm joos} \rangle = (1.4 \pm 0.8) \cdot 10^{-3} \tag{30}$$

and a corresponding observable velocity $v_{\rm obs} \sim 1.8^{+0.5}_{-0.6}$ km/s. By correcting with the helium refractive index, Eq.(11) would then imply a true kinematical velocity $v \sim 217^{+66}_{-79}$ km/s.

However, this is only a first and very partial view of Joos' experiment. In fact, we have compared Joos' amplitudes with theoretical models of cosmic motion. To this end, after transforming the civil times of Joos' measurements into sidereal times, by using Eqs.(15) and (18), one can compare

Joos' amplitudes with theoretical predictions which, for the given latitude $\phi = 50.94$ degrees of Jena, depend on the right ascension α and the angular declination γ. To this end, it is convenient to first re-write the theoretical forms as

$$A_2(t)\cos 2\theta_0(t) = 2C(t) = \frac{2L(\mathcal{N}-1)}{\lambda}\,\frac{v_x^2(t)-v_y^2(t)}{c^2} \sim 2.6{\cdot}10^{-3}\,\frac{v_x^2(t)-v_y^2(t)}{(300\ \mathrm{km/s})^2} \tag{31}$$

and

$$A_2(t)\sin 2\theta_0(t) = 2S(t) = \frac{2L(\mathcal{N}-1)}{\lambda}\,\frac{2v_x(t)\ v_y(t)}{c^2} \sim 2.6{\cdot}10^{-3}\,\frac{2v_x(t)\ v_y(t)}{(300\ \mathrm{km/s})^2} \tag{32}$$

where we have used the numerical relation for Joos's experiment $\frac{L}{\lambda}\,\frac{(30\mathrm{km/s})^2}{c^2} \sim 0.375$ and the value of the helium refractive index. Then, by approximating $v_x(t) \sim \tilde{v}_x(t)$, $v_y(t) \sim \tilde{v}_y(t)$ and using Eq.(18) for the scalar combination $\tilde{v}(t) \equiv \sqrt{\tilde{v}_x^2(t)+\tilde{v}_y^2(t)}$, we have fitted the data of Fig.6 to the smooth form

$$A_2^{\mathrm{smooth}}(t) = \mathrm{const}\cdot \sin^2 z(t) \tag{33}$$

where $\cos z(t)$ is defined in Eq. (15). The results of the fit

$$\alpha = 168^o \pm 30^o \qquad\qquad \gamma = -13^o \pm 14^o \tag{34}$$

confirm that, as found in connection with the Michelson-Morley experiment, the Earth's motion with respect to the CMB (which has $\alpha \sim 168^o$ and $\gamma \sim -6^o$) could serve as a useful model to describe the ether-drift data.

Still, in spite of the good agreement with the CMB $\alpha-$ and $\gamma-$values obtained from the fit Eq.(34), the nature of the strong fluctuations in Fig.6 remains unclear. Apart from this, there is also a sizeable discrepancy in the absolute normalization of the amplitude. In fact, by assuming the standard picture of smooth time modulations, the mean amplitude over all sidereal times can trivially be obtained from the mean squared velocity Eq.(18)

$$\langle \tilde{v}^2(t)\rangle = V^2\left(1-\sin^2\gamma\sin^2\phi-\frac{1}{2}\cos^2\gamma\cos^2\phi\right) \tag{35}$$

For the CMB and Jena, this gives $\sqrt{\langle\tilde{v}^2\rangle} \sim 330$ km/s so that one would naively predict from Eqs.(31), (32)

$$\langle A_2^{\mathrm{smooth}}(t)\rangle \sim 2.6\cdot 10^{-3}\ \frac{\langle\tilde{v}^2(t)\rangle}{(300\ \mathrm{km/s})^2} \sim 3.2\cdot 10^{-3} \tag{36}$$

to be compared with Joos' mean value $\langle A_2^{\mathrm{joos}}\rangle = (1.4\pm 0.8)\cdot 10^{-3}$. In the standard picture, this experimental value leads to the previous estimate

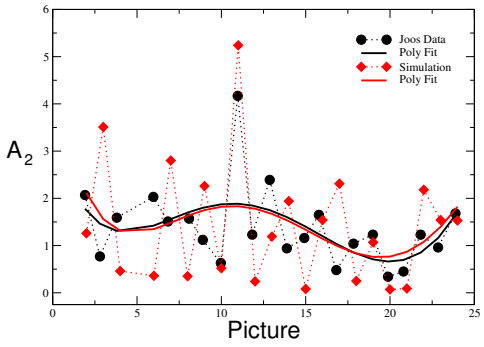

Fig. 7. Joos' experimental amplitudes in Fig.6 are compared with a single simulation of 22 instantaneous measurements. By changing the random sequence, the typical variation of each simulated entry is $(1 \div 4) \cdot 10^{-3}$ depending on the sidereal time. The stochastic velocity components are controlled by the kinematical parameters $(V, \alpha, \gamma)_{\rm CMB}$ as explained in the text. We also show two 5th-order polynomial fits to the two different sets of values. The figure is taken from Ref.[39].

$\sqrt{\langle \tilde{v}^2 \rangle} \sim 217$ km/s and *not* to $\sqrt{\langle \tilde{v}^2 \rangle} \sim 330$ km/s so that it is necessary to change the theoretical model to try to make Joos' experiment completely consistent with the Earth's motion with respect to the CMB.

To try to solve this problem, and understand the origin of the observed strong fluctuations, we have used the model Eqs.(26), (27) of Sect.6, to simulate stochastic variations of the velocity field. As anticipated, due to the high accuracy of the Joos experiment, the two random parameters $x_n(1)$ and $x_n(2)$ were allowed to vary in the range $[-\tilde{v}_x(t), \tilde{v}_x(t)]$ and the other two parameters $y_n(1)$ and $y_n(2)$ to vary in the different range $[-\tilde{v}_y(t), \tilde{v}_y(t)]$, where $\tilde{v}_x(t)$ and $\tilde{v}_y(t)$ are defined in Eqs.(15)−(17). Also the quadratic values were fixed as in Eqs.(29). It is understood that the latitude corresponds to Joos' experiment while V, α and γ describe the Earth's motion with respect to the CMB.

In this model, there will be a substantial reduction of the amplitude with respect to its smooth prediction. To estimate the order of magnitude of the reduction, one can perform a full statistical average (as for an infinite number of measurements) and use Eqs.(29) in Eqs.(31), (32) for our case $\eta = 1$. This gives

$$\langle A_2(t) \rangle_{\rm stat} \sim 2.6 \cdot 10^{-3} \, \frac{\tilde{v}^2(t)}{(300 \text{ km/s})^2} \, \frac{1}{3} \sum_{n=1}^{\infty} \frac{1}{n^2} = \frac{\pi^2}{18} \, A_2^{\rm smooth}(t) \qquad (37)$$

By also averaging over all sidereal times, for the CMB and Jena, one would now predict a mean amplitude of about $1.7 \cdot 10^{-3}$ and not of $3.2 \cdot 10^{-3}$.

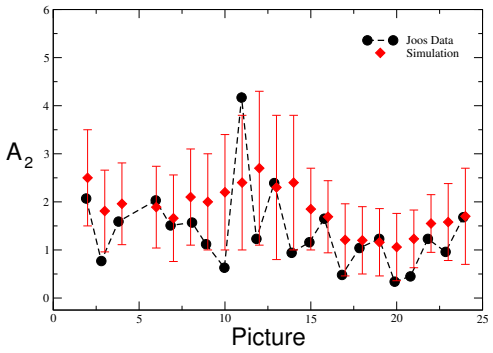

Fig. 8. Joos' experimental amplitudes in Fig.6 are compared with the result of simulating the averaging process over 10 measurements performed, at each Joos' time, on 10 consecutive days. The stochastic velocity components are controlled by the kinematical parameters $(V, \alpha, \gamma)_{\rm CMB}$ as explained in the text. The effect of varying the random sequence has been approximated into a central value and a symmetric error. The figure is taken from Ref.[39].

To have an idea of the agreement between Joos' 22 amplitude data and a *single* numerical simulation of instantaneous measurements, we show a graphical comparison in Fig. 7. We emphasize that one should not compare each individual entry with the corresponding data since, by changing the random sequence, the simulated instantaneous entries vary typically of about $(1 \div 4) \cdot 10^{-3}$ depending on the sidereal time. Instead, one should compare the overall trend of data and simulation. To this end, we show two 5th-order polynomial fits to the two different sets of values.

A more conventional comparison with the data consists in quoting for the various 22 entries simulated average values and uncertainties. To this end, we have considered the mean amplitudes $\langle A_2^{\rm simul}(t_i)\rangle$ defined by averaging, for each Joos' time t_i, over 10 hypothetical measurements performed on 10 consecutive days. For each t_i, the observed effect of varying the random sequence has been summarized into a central value and a symmetric error. The simulated values and the comparison with Joos' amplitudes is shown in Fig.8.

The spread of the various entries is larger at the sidereal times where the projection at Jena of the cosmic Earth's velocity becomes larger. The tendency of Joos' data to lie in the lower part of the simulated range mostly depends on our use of symmetric errors. In fact, by comparing in some case with the histograms of the basic generated configurations $A_2^{\rm simul}(t_i)$, we have seen that our sampling method of $\langle A_2^{\rm simul}(t_i)\rangle$ typically underestimates

the weight of the low-amplitude region in a prediction at the 70% C.L.. For this reason, one could improve the evaluation of the probability content. However, in view of the good agreement already found in Fig.8 ($\chi^2 = 13/22$), we did not attempt to carry out this more refined analysis.

In conclusion, after the first indication obtained from the fit Eq.(34), the link between Joos' data and the Earth's motion with respect to the CMB gets reinforced by our simulations. In fact, by inspection of Figs.7 and 8, the values of the amplitudes and the characteristic scatter of the data are correctly reproduced. From this agreement, we then deduce that the previous kinematical value $v \sim 217^{+66}_{-79}$ km/s has to be considerably increased if one allows for stochastic variations of the velocity field. In fact, the magnitude of the fluctuations in v_x and v_y is controlled by the same scalar parameter $\tilde{v}(t) \equiv \sqrt{\tilde{v}_x^2(t) + \tilde{v}_y^2(t)}$ of Eq.(18). We thus conclude that Joos' data are consistent with a range of kinematical velocity $v = 330^{+40}_{-70}$ km/s which corresponds to Eq.(18) for $\phi = 50.94^o$, $V = 370$ km/s, $\alpha = 168^o$ and $\gamma = -6^o$.

6. Summary and conclusions

Traditionally, the interpretation of the ether-drift experiments has been based on a theoretical model where all type of signals that are not synchronous with the Earth's rotation tend to be considered as spurious instrumental noise. However, there is a logical gap. The link between the two concepts depends on the adopted model for the vacuum. The point of view adopted so far corresponds to consider the vacuum as some kind of fluid in a state of regular, laminar motion. In these conditions global and local properties of the flow coincide.

We believe that, without fully understanding the nature of that substratum that we call physical vacuum, one should instead keep a more open mind. As discussed in Sect.2, the physical vacuum might be similar to a form of turbulent ether, an idea which is deep rooted in basic foundational aspects of both quantum theory and relativity and finds additional motivations in those representations of the vacuum as a form of 'space-time foam' which indeed resembles a turbulent fluid. In this case, *global* and *local* velocity fields might be very different and there could be forms of random signals that have a genuine physical origin.

To explore this idea, we have re-considered from scratch the classical experiments. These were performed in gaseous media where the refractive

Experiment	gas in the interf.	$v_{\rm obs}$(km/s)	v(km/s)
Mich.-Morley(1887)	air	$8.4^{+1.5}_{-1.7}$	349^{+62}_{-70}
Mor.-Miller(1902-1905)	air	8.5 ± 1.5	353 ± 62
Kennedy(1926)	helium	< 5	< 600
Illingworth(1927)	helium	3.1 ± 1.0	370 ± 120
Miller(1925-1926)	air	$8.4^{+1.9}_{-2.5}$	349^{+79}_{-104}
Mich.-Pease-Pearson(1929)	air	$4.5 \pm ...$	$185 \pm ...$
Joos(1930)	helium	$1.8^{+0.5}_{-0.6}$	330^{+40}_{-70}

index $\mathcal{N}$ is extremely close to unity. In this case, in the framework of a Lorentzian view of relativity, by expanding around $\mathcal{N} = 1$ and to leading order in v/c, one formally finds the same classical formulas with the only replacement

$$v^2 \to 2(\mathcal{N} - 1)v^2 \equiv v^2_{\rm obs} \tag{38}$$

As discussed in detail in Sect.3, this replacement can be understood with simple symmetry arguments but also admits a dynamical interpretation in terms of the energy-momentum flow associated with a Lorentz non-invariant vacuum. As emphasized in Sect.3, this dynamical mechanism is not unexpected on the basis of the present views of the vacuum as a particle condensate and is also useful to reconcile the different phenomenological pattern between ether-drift experiments in gaseous media and those performed in strongly bound systems such as solid or liquid transparent media.

Now testing the scheme is very simple: one should just check the consistency of the true kinematical v's obtained in different experiments. In this alternative interpretation, the indications of the various experiments are summarized in our Table 2 which is taken from ref.[39] (to which we address the reader for many details). Here, we just emphasize the following points:

i) an analysis of the individual sessions of the original Michelson-Morley experiment, in agreement with Hicks [49] and Miller [48] (see our Figs. 1 and 2), gives no justification to its standard null interpretation. As discussed in Sect.5, this type of analysis is more reliable. In fact, averaging directly the fringe displacements of different sessions requires two additional assumptions, on the nature of the ether-drift as a smooth periodic effect and on the absence of systematic errors introduced by the re-adjustment of the mirrors on consecutive days, that in the end may turn out to be wrong.

ii) from the Michelson-Morley, Morley-Miller, Miller and Illingworth-

Kennedy experiments one gets average kinematical velocities which are well consistent with the value 370 km/s which today is used to describe the CMB anisotropy. In view of this consistency, the standard interpretation of Miller's observations in terms of a temperature gradient [51] is only acceptable provided this gradient represents a non-local effect as in the picture of [39; 40] where the ether-drift is the consequence of a fundamental vacuum energy-momentum flow.

iii) some discrepancy is found with the experiment performed by Michelson, Pease and Pearson (MPP). At the same time, as emphasized in [39], the uncertainty cannot be easily estimated since only a single basic MPP observation is explicitly reported in the literature. Therefore, since Miller's extensive observations (see Fig.22 of ref.[48]), within their errors, gave fluctuations of the observable velocity in the wide range $4-14$ km/s, a single observation giving $v_{\rm obs} \sim 4.5$ km/s cannot be interpreted as a refutation. This becomes even more true by noticing that the single MPP session explicitly reported, within a period of several months, was chosen to represent an example of extremely small ether-drift effect.

iv) Joos' experiment is particularly important since the data were collected at steps of 1 hour to cover the full sidereal day and were recorded by photocamera. For this reason, it is not comparable with other experiments (e.g. Michelson-Morley, Illingworth) where only observations at few selected hours were performed and for which, in view of the strong fluctuations of the data, one can just quote the average magnitude of the observed velocity. In fact, by fitting the experimental amplitudes in Fig.6 to various forms of cosmic motion (see Eq.(34)) we have obtained angular parameters which are very close to those that describe the CMB anisotropy (right ascension $\alpha_{\rm CMB} \sim 168^o$ and angular declination $\gamma_{\rm CMB} \sim -6^o$). Still, to get a complete agreement, one should explain the absolute normalization of the amplitudes and the strong fluctuations of the data. Thus we have sharpened our analysis by performing various numerical simulations where the velocity components $v_x(t)$ and $v_y(t)$ are not smooth functions but are represented as turbulent fluctuations. Their Fourier components in Eqs.(26) and (27) vary within time-dependent ranges Eqs.(16)$-$(17), $[-\tilde{v}_x(t), \tilde{v}_x(t)]$ and $[-\tilde{v}_y(t), \tilde{v}_y(t)]$ respectively, controlled by the macroscopic parameters $(V, \alpha, \gamma)_{\rm CMB}$. Taking into account these stochastic fluctuations of the velocity field tends to increase the fitted average Earth's velocity, see Eq.(37), and can reproduce correctly Joos' 2nd-harmonic amplitudes and the characteristic scatter of the data, see Figs. 7 and 8.

These results, give a strong motivation to repeat these crucial measure-

ments with today's much greater accuracy. To this end, let us now briefly consider the modern ether-drift experiments. In this case, the test of the isotropy of the velocity of light consists in measuring the relative frequency shift $\Delta\nu$ of two orthogonal optical resonators [58]. Here, the analog of Eq.(10) is

$$\frac{\Delta\nu^{\rm phys}(\theta)}{\nu_0} = \frac{\bar{c}_\gamma(\pi/2+\theta) - \bar{c}_\gamma(\theta)}{c} = \mathcal{B}_{\rm medium}\frac{v^2}{c^2}\cos 2(\theta-\theta_0) \qquad (39)$$

where θ_0 is the direction of the ether-drift. This can be interpreted within Eq.(8) where

$$|\mathcal{B}_{\rm medium}| \sim \mathcal{N}_{\rm medium} - 1 \qquad (40)$$

$\mathcal{N}_{\rm medium}$ being the refractive index of the gaseous medium filling the optical resonators. Testing this prediction, requires replacing the high vacuum usually adopted within the optical resonators with a gaseous medium and studying the substantially larger frequency shift introduced with respect to the vacuum experiments.

As a rough check, a comparison was made [41; 42] with the results obtained by Jaseja et. al [59] in 1963 when looking at the frequency shift of two orthogonal He-Ne masers placed on a rotating platform. To this end, one has to preliminarily subtract a large systematic effect that was present in the data and interpreted by the authors as probably due to magnetostriction in the Invar spacers induced by the Earth's magnetic field. As suggested by the same authors, this spurious effect, which was only affecting the normalization of the experimental $\Delta\nu$, can be subtracted by looking at the variations of the data. As discussed in refs.[41; 42], the measured variations of a few kHz are roughly consistent with the refractive index $\mathcal{N}_{\rm He-Ne} \sim 1.00004$ and the typical variations of an Earth's velocity as in Eq.(25).

More recent experiments [60]−[64] have always been performed in a very high vacuum where, as emphasized in the Introduction, the differences between Special Relativity and the Lorentzian interpretation are at the limit of visibility. In fact, in a perfect vacuum by definition $\mathcal{N}_{\rm vacuum} = 1$ so that $\mathcal{B}_{\rm vacuum}$ will vanish [e]. Thus one should switch to the new generation of dedicated ether-drift experiments in gaseous systems. Our conclusion is that

[e]Strictly speaking, modern experiments in vacuum are also consistent with an instantaneous ether-drift effect of order 10^{-15}. In the framework of Eq.(7), for values $v^2/c^2 \sim 10^{-6}$, this could indicate that the velocity of light in the vacuum, as measured on the Earth's surface, differs from the parameter c entering Lorentz transformations at the level $\mathcal{O}(10^{-9})$. A possible theoretical scenario for this difference, after incorporating the idea of vacuum turbulence [65; 66], is completely consistent with the present data.

these new experiments should just confirm Joos' remarkable observations of eighty years ago.

References

1. C. D. Froggatt and H. B. Nielsen; "*Origin of Symmetries*", World Scientific, 1991.
2. *Physics Of Emergence And Organization*, I. Licata and A. Sakaji Eds.; World Scientific 2008.
3. E. T. Whittaker; "*A history of the Theories of Aether and Electricity*", Dover Publ. 1989.
4. O. V. Troshkin; Physica **A168** (1990) 881.
5. H. E. Puthoff; "*Linearized turbulent flow as an analog model for linearized General Relativity*", arXiv:0808.3404 [physics.gen-ph].
6. T. D. Tsankov; "*Classical Electrodynamics and the Turbulent Aether Hypothesis*", Preprint February 2009.
7. M. J. Marcinkowski; "*Physica Status Solidi*"**152B** (1989) 9.
8. A. M. Kosevic; "*The Crystal Lattice: Phonons, Solitons, Superlattices*", Wiley-VCH Verlag Gmbh and Co. KGaA, Weinheim 2005.
9. H. Günther; "*Physica Status Solidi*", **149** (1988) 104.
10. C. I. Christov; "*Math. Comput. Simul.*", **74** (2007) 93.
11. R. P. Feynman, R. B. Leighton and M. Sands; "*The Feynman Lectures on Physics*", Addison Wesley Publ. Co. 1963, Vol.I, Sect. 15.9.
12. M. Consoli; Phys. Lett. **A 376** , 3377 (2012).
13. M. Consoli, A. Pluchino and A. Rapisarda; Chaos, Solitons and Fractals **44**, 1089 (2011).
14. T. W. Marshall; Proc. R. Soc. A **276** (1963) 475.
15. T. H. Boyer; Phys. Rev. **182** (1969) 1374; *ibidem* **186** (1969) 1304.
16. H. E. Puthoff; Phys. Rev. D **35** (1987) 3266.
17. L. de la Peña and A. M. Cetto; "*The Quantum Dice - An Introduction to Stochastic Electrodynamics*", Kluwer Academic Publ., Dordrecht 1996.
18. D. C. Cole and Y. Zou; Phys. Lett. A **317** (2003) 14.
19. E. Nelson; Phys. Rev. **150** (1966) 1079.
20. L. Onsager; Nuovo Cimento, Suppl. **6** (1949) 279.
21. A. N. Kolmogorov; Dokl. Akad. Nauk SSSR **30** (1940) 4.
22. P. Jizba and H. Kleinert; Phys. Rev. **D82** (2010) 085016.
23. P. Jizba and F. Scardigli; "*Special Relativity induced by Granular Space*", arXiV:1301.4091v2[hep-th].
24. C.Beck and E.G.D.Cohen; Physica A **322** (2003) 267.
25. C. Beck; Phys. Rev. Lett. **98**, 064502 (2007).
26. J. A. Wheeler; in "*Relativity, Groups and Topology*", B. S. DeWitt and C. M. DeWitt Eds., Gordon and Breach New York 1963, p. 315.
27. S. Hawking; Nucl. Phys. **B144**, 349 (1978).
28. R. Bousso; Rev. Mod. Phys. **74**, 825 (2002).
29. G. Amelino-Camelia; Nature **418** (2002) 34.

30. Y. J. Ng; "*Various Facets of Spacetime Foam*", in Proceedings of the Third Conference on Time and Matter, Budva, Montenegro 2010, arXiv:1102.4109 [gr-qc].
31. Y. J. Ng and H. van Dam; Mod. Phys. Lett. **A9**, 335 (1994).
32. M. T. Jaekel and S. Reynaud; Phys. Lett. **A185**, 143 (1994).
33. E. Göklü and C. Lämmerzahl; Class. Quant. Grav. **25**, 105012 (2008).
34. E. Göklü et al.; Class. Quant. Grav. **26**, 225010 (2009).
35. G. Amelino-Camelia; Phys. Rev. **D62**, 024015 (2000).
36. E. Göklü and C. Lämmerzahl; Gen. Rel. Grav. **43**, 2065 (2011).
37. S. Schiller et al.; Phys. Rev. **D69**, 027504 (2004).
38. V. Jejjala, D. Minic, Y. J. Ng and C. H. Tze; Int. J. Mod. Phys. **D19** (2010) 2311.
39. M. Consoli, C. Matheson and A. Pluchino; Eur. Phys. J. Plus **128**, 71 (2013).
40. M. Consoli and E. Costanzo; Eur. Phys. Journ. **C54** (2008) 285.
41. M. Consoli and E. Costanzo; Phys. Lett. **A333** (2004) 355.
42. M. Consoli and E. Costanzo; N. Cim. **119B** (2004) 393.
43. J. Shamir and R. Fox; N. Cim. **62B**, 258 (1969).
44. H. A. Lorentz; "*The Theory of Electrons*", Leipzig 1909, B. G. Teubner Ed.
45. H. P. Robertson; Rev. Mod. Phys. **21**, 378 (1949).
46. R. M. Mansouri and R. U. Sexl; Gen. Rel. Grav. **8**, 497 (1977).
47. A. A. Michelson and E. W. Morley; Am. J. Sci. **34** (1887) 333.
48. D. C. Miller; Rev. Mod. Phys. **5** (1933) 203.
49. W. M. Hicks; Phil. Mag. **3** (1902) 9.
50. M. Born; "*Einstein's Theory of Relativity*", Dover Publ., New York, 1962.
51. R. S. Shankland et al.; Rev. Mod. Phys., **27**, (1955) 167.
52. M. A. Handshy; Am. J. of Phys. **50** (1982) 987.
53. L. D. Landau and E. M. Lifshitz; "*Fluid Mechanics*", Pergamon Press 1959, Chapt. III.
54. J. C. H. Fung et al.; J. Fluid Mech. **236**, 281 (1992).
55. G. Joos; Ann. d. Physik **7** (1930) 385.
56. Loyd S. Swenson Jr.; Journ. for the History of Astronomy, **1**, 56 (1970).
57. K. K. Illingworth; Phys. Rev. **30** (1927) 692.
58. Special Relativity, J. Ehlers and C. Lämmerzahl Eds.; " *Lectures Notes in Physics*", Springer 2006.
59. T. S. Jaseja, et al.; Phys. Rev. **133** (1964) A1221.
60. A. Brillet and J. L. Hall; Phys. Rev. Lett. **42** (1979) 549.
61. P. Antonini, et al.; Phys. Rev. **A71**, 050101(R)(2005).
62. S. Herrmann, et al.; Phys. Rev. Lett. **95**, 150401 (2005).
63. S. Herrmann, et al.; Phys.Rev. D **80**, 105011 (2009).
64. Ch. Eisele, A. Newski and S. Schiller; Phys. Rev. Lett. **103**, 090401 (2009).
65. M. Consoli and L. Pappalardo; Gen. Rel. and Grav. **42**, 2585 (2010).
66. M. Consoli, A. Pluchino, A. Rapisarda and S. Tudisco; Physica A**394**, 61 (2014).